DISCRETE AND CONTINUOUS
DYNAMICAL SYSTEMS–SERIES B
Volume **3**, Number **2**, May **2003**

Website: http://www.aimsciences.org/dcdsB.htm

pp. **263–284**

CHAOTIC ADVECTION, TRANSPORT AND PATCHINESS IN CLOUDS OF POLLUTION IN AN ESTUARINE FLOW

J.R. Stirling

Departament de Matemàtica Aplicada I,
Universitat Politècnica de Catalunya,
Diagonal 647, E-08028 Barcelona, Spain.

(Communicated by Angel Jorba)

Abstract. We present an application of the transport theory developed for area preserving dynamical systems, to the problem of pollution and in particular patchiness in clouds of pollution in partially stratified estuaries. We model the flow in such estuaries using a $3+1$ dimensional uncoupled cartoon of the dominant underlying global circulation mechanisms present within the estuarine flow. We separate the cross section up into different regions, bounded by partial and complete barriers. Using these barriers we then provide predictions for the lower bound on the vertical local flux. We also present work on the relationship between the time taken for a particle to leave the estuary, (ie. the exit time), and the mixing within the estuary. This link is important as we show that to optimally discharge pollution into an estuary both concepts have to be considered. We finish by suggesting coordinates in space time for an optimal discharge site and a discharge policy to ensure the continually optimal discharge from such a site (or even a non optimal site).

1. **Introduction.** In this paper we present an application of transport theory (see [21, 31, 11, 14, 12]) and chaotic advection (see [1, 2, 16]) to the transport and patchiness of pollution in a partially stratified estuary. An understanding of the dynamics of pollution released into such flows is of fundamental importance as many large industrial developments and cities are focussed about such flows. Estuaries are used for a wide variety of activities including waste disposal, providing drinking water, recreation, transport and power plant cooling. As could be imagined, a poor understanding of the mixing could have severe consequences. As in [17, 20, 27, 28] we model the estuarine flow with a set of coupled ordinary differential equations which describe the underlying dynamics of the estuarine flow. Our model is based on a set of circulations, (see figure 1) proposed in [23] (see also [22]) to model the buoyancy driven circulations in an estuarine flow. These are transverse circulations caused by the density difference between the fresh river water and the salty sea water. During the ebb tide the water in the center of the estuary is fresher (lower salinity) and hence is less dense than the more salty water at the sides of the estuary. During the flood tide the flow changes direction and hence the water in the center of the estuary is more salty than that at the edges. This results in the presence of the time periodic transverse double circulation cell for the buoyancy driven flow in the YZ plane. The existence of these circulations was verified practically in

1991 *Mathematics Subject Classification.* 37, 76.
Key words and phrases. Chaos, transport, lobe dynamics, pattern formation, pollution.

[9, 10, 15, 30]. For the secondary circulation or transverse velocity field ($\mathcal{V}_f$ and $\mathcal{W}_f$) we use a set of Hamiltonian equations obtained from a stream function Ψ_f presented in [28]. We add to these equations, an uncoupled velocity field $\mathcal{U}_f$, in the along estuary direction X, where $\mathcal{U}_f$ is a function of Y, Z, and t only.

We consider the evolution of a cloud of pollution discharged into such an estuary as described by our model. One of the major questions is, *what is the environmental impact of such a cloud?* The impact is governed by the peak concentration of the cloud, and not its average, which is calculated in the standard approach to this question. (For a review see [4, 7, 8, 26].) If there are trapping regions within the cloud, then the concentration and flux associated with such regions are of fundamental importance. As was explained in [27, 28], it is observed that within a typical cloud of pollution there are large to medium scale patches of different concentration. (See [19, 5, 29] for practical observations of patchiness in estuarine and coastal flows.) We associate such patchiness with trapping regions formed as a result of the large scale global dynamics of the flow. The other main question of interest is, *what are the optimal discharge positions, within the space-time coordinates of the estuary, for the release of pollution?* We provide answers to this question via calculations of the flux in the vertical plane and the time taken to exit from the two open ends of the estuary. By optimizing these two parameters and understanding the Stokes drift we provide optimal discharge site coordinates. These values of exit times could also be used to help explain such things as the reason why mud remains in an estuary and does not get flushed out. We present two general results with regards the exit times in 3-dimensional time dependent flows. The first result is that *the complete and partial barriers do not only separate regions of different mixing, they also separate regions of different Stokes drift and hence different exit times.* The second result is that *regions in which the mixing is good and with boundaries which extend close to those of the fluid are regions of long exit time, for flows with non slip boundary conditions.* (It is also shown that the converse of this second result is true, i.e. regions of poor mixing, with boundaries remain far from those of the fluid are regions of short exit time, for flows with non slip boundary conditions.) We also show the importance of the Stokes drift and how, by discharging in the wrong place, it is possible for the pollution to drift back against the flow of the estuary. The environmental impact of such an event could be severe.

The presence of negative Stokes drift and patchiness shows the need for a full or more complete treatment of pollution before it is discharged and enters the estuary. This is because the trapping regions which cause the patchiness do not allow for the dispersion of pollutants via stirring. The only means of escape from such regions is via diffusion (i.e. turbulent and molecular). Secondly, such regions are often associated with a positive or, more importantly, a negative Stokes drift. This negative Stokes drift has the effect of keeping the pollution in such a region at a high concentration whilst with increasing tidal periods the pollution will drift back upstream, where it came from. Both these effects support our claim regarding the treatment of the pollution. As was discussed in [27, 28], the standard averaged approach to modelling does not account for such regions and therefore we claim that such approaches could have a serious potential to underestimate the impact of a cloud of pollution by not attempting to model the peak concentrations. As a side issue it has to be noted that [27, 28] carries an even worse message. In a model we

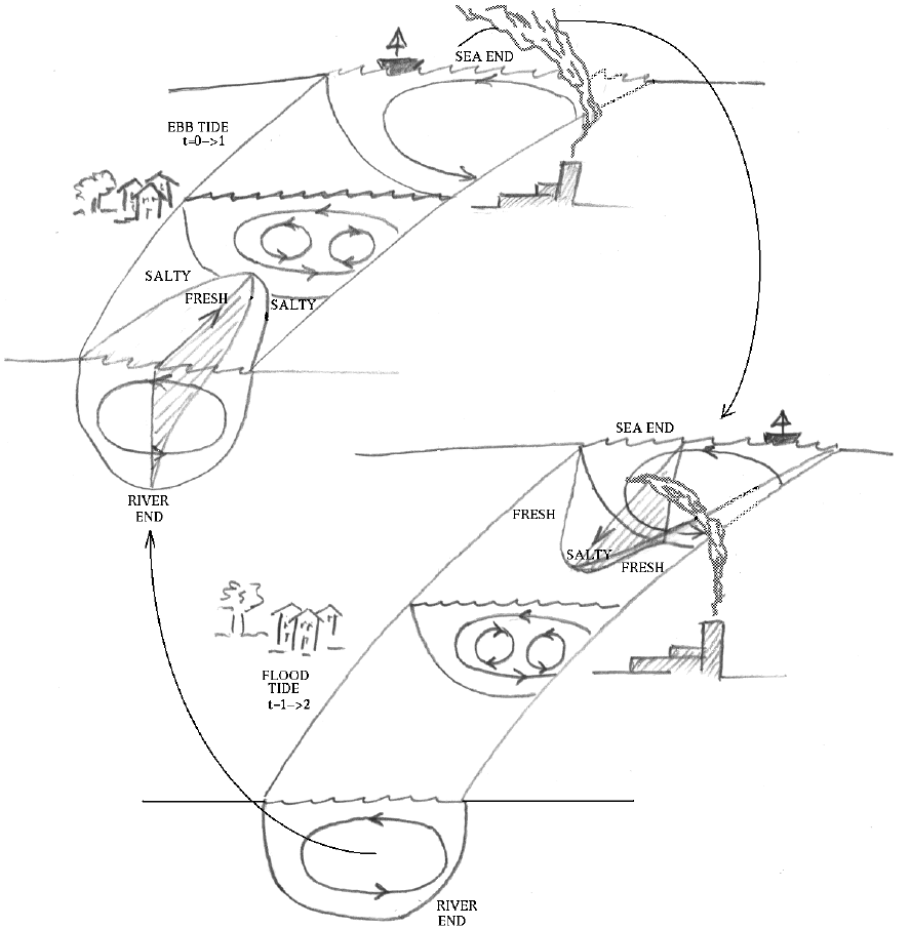

FIGURE 1. Cartoon of the periodic flow in an estuary, for both the ebb and flood phases of the tide, showing the transverse secondary circulation in the vertical cross section via both the single cell (wind or bend-driven) and the periodic double cell (density driven). We also show how the X directional (along estuary) velocity profile varies with Y (the transverse direction to the flow), Z (the vertical direction) and the direction of the tide. See figure 2 for the coordinate axis.

developed there, not only do we get negative Stokes drift and trapping regions, but the trapping regions can also be regions of attraction.

In the following sections of this paper we first present the equations we use to model the estuarine flow, and the equations governing the underlying dynamics in the estuarine flow (i.e. v_f). We also present how our model can be scaled up to suitable estuarine dimensions, and some of the assumptions we have made. In the third section we show how the full 3-dimensional Poincaré map is obtained. We also show how a vertical cross section can be split up into different regions, and finish by linking this in with patches and patchiness in clouds of pollution in an estuarine flow. The fourth section is about the effect of the third dimension X.

We first introduce the concept of Stokes drift and show how this links in with the concept of a map. We then go onto explain how the barriers observed in the YZ Poincaré map will appear when seen in the full 3 dimensional time periodic flow. Section 5 presents the predicted values for the flux, both in our model and in the estuary. This section also includes a subsection on exit times, and is one of the most important parts of the paper. In it we present our results regarding the link between the exit times and the mixing. Section 6, applies the results presented in section 5, to the problem of pollution discharges into the estuary. In the first part we present the practical implications of the predicted diffusion rates we obtained from our model of the turbulent flow. Using this information we then suggest an optimal discharge region in the vertical cross section. We finish the section by providing optimal discharge coordinates in space (i.e. XYZ coordinates) and discussing the need for suitable discharge policies to keep these coordinates optimal through out the whole tidal period.

2. **Introduction to the model.** Here we first present the assumptions we have made in our model and then we present the fundamental velocity field, v_f, of the estuarine flow. We refer to v_f as the cartoon. v_f is that part of the velocity field V which dominates the large scale global dynamics of the estuarine flow, (ie. $v_f = V - v'$ where v' is the essentially random part of the turbulent flow). We then go on to discuss solutions found on the boundaries of the estuary.

2.1. **The material exiting out of sea and river end, and other assumptions.** In our model, material can exit out of both the sea and the river end of our estuary, hence the reason why the domain is not bounded in the X direction. We make two assumptions regarding this, the first is that the material which leaves through the sea end does not come back into the system, and secondly the material leaving through the river end is re-injected back into the estuary, though we do not state where. These are fairly realistic assumptions if we also make the assumption that the material entering into the river can only move in the direction of the river flow as there is no tidal oscillation. It is standard to think of and treat the estuary and the coastal sea as separate entities.

We also make the assumption that the coupling between the X and Y, Z directional velocity fields is nonexistent or very weak (i.e. essentially zero).This allows us to uncouple the equations governing the flow in the X direction from those governing the flow in the transverse YZ direction. There are two obvious situations were this is valid. The first is the sort of situation where the flows dynamics does not change sufficiently with X to consider its inclusion important in the model. Flow along a regular shaped channel would be a good example of this. (See [27, 28] for the case where the flow does change with X.) The second situation is flow along a self similar channel. See the paper [24] for examples of such channel shapes.

2.2. **The large scale or fundamental velocity field, v_f.** Figure 1 shows the circulations in our estuary. These are the dominant large scale global circulation mechanisms which underly our flow. In this section we consider the equations of v_f. They describe a velocity field which has the same large scale global circulation mechanisms as were originally predicted in [23] to underly an estuarine flow on a bend (i.e. a double circulation cell surrounded by a single circulation cell). The X directional flow in an estuary is to a good approximation periodic with the period being that of the tide (i.e. $T = 2$). The periodicity in the along estuary velocity field $\mathcal{U}_f = \dot{X}$ models this periodic change in direction and magnitude of the X

directional along estuary tidal flow resulting from the periodic change in direction of the tide. The periodicity can be seen in figure 1 where the X directional along estuary flow is from the river to the sea end during the ebb tide whilst during the flood tide the direction of the flow is reversed and hence is from the sea to the river end of the estuary. As explained earlier this periodicity in the along estuary directional flow combined with shape of the X directional velocity profile and the density difference between fresh and salty water results in a periodic double cell buoyancy driven circulation, see figure 1. The horizontal $\mathcal{V}_f = \dot{Y}$ and vertical $\mathcal{W}_f = \dot{Z}$ velocity fields therefore both contain periodic functions of time, which model the periodic changes in the double cell buoyancy driven circulation.

As stated earlier our model, and hence the domain, is unbounded in the X direction, though we consider that when a trajectory leaves the bounds $-1 \leq X \leq 1$ in the flow, it has left the estuary, and therefore we are not interested in it anymore. The bounds on the other dimensions are $-1 \leq Y \leq 1$ and $-1 \leq Z \leq 0$, see figure 2.

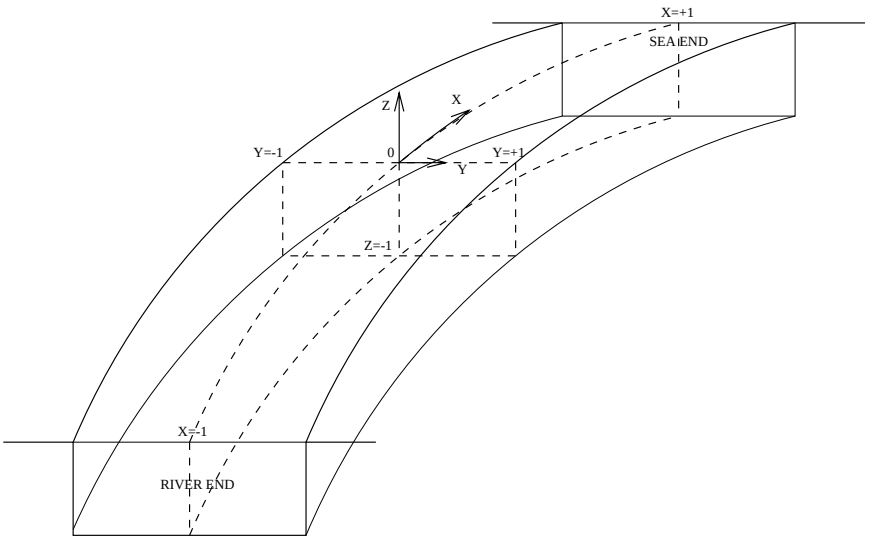

FIGURE 2. The coordinate axis and bounds of our estuary.

The following equations (i.e. 2 to 4) are a modification of those presented in [27, 28], such that $\mathcal{U}_f$ is uncoupled from both $\mathcal{V}_f$ and $\mathcal{W}_f$. In this set of equations, R is the ratio of the river's component of the velocity field to that of the tide, L is a parameter which measures the relative strengths of the longitudinal circulation to the transversal circulation and the parameter K is a measure of the relative strengths of the buoyancy driven to the bend driven circulation, in the vertical YZ cross section.

The stream function ψ_f (see figure 3 for plots of ψ_f for different times during the tidal period) is used to model the flow in the vertical YZ cross section:

$$\psi_f = (1 - Y^2)Z(1 + Z)^2(1 + KY \sin(\pi t)). \tag{1}$$

This gives

$$\mathcal{V}_f = \dot{Y} = -\frac{\partial \psi_f}{\partial Z} = (3Z + 1)(Z + 1)(Y^2 - 1)(1 + KY \sin(\pi t)), \tag{2}$$

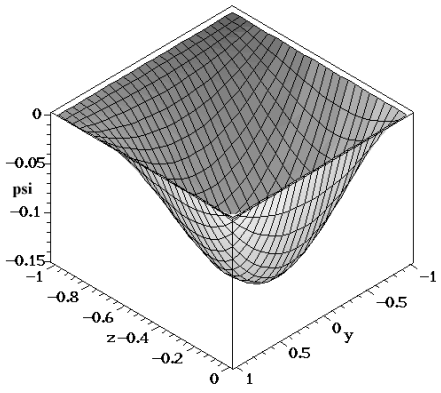

(a)ψ_f p n, $n \in \mathbb{N}$

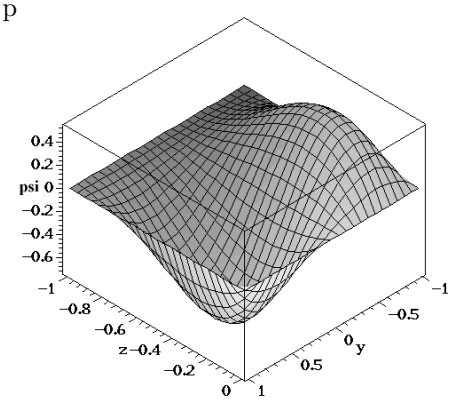

(b)ψ_f plotted against YZ for $K = 11$ and $t = 0.5 + 2n$, $n \in \mathbb{N}$

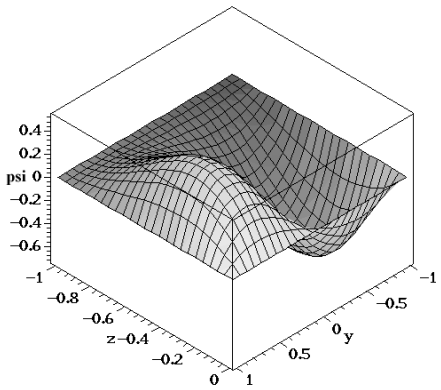

(c)ψ_f plotted against YZ for $K = 11$ and $t = 1.5 + 2n$, $n \in \mathbb{N}$

FIGURE 3. A plot of the stream function ψ_f for different times during the tidal period.

$$\mathcal{W}_f = \dot{Z} = \frac{\partial \psi_f}{\partial Y} = Z(1+Z)^2((1-3Y^2)K\sin(\pi t) - 2Y). \tag{3}$$

For $\mathcal{U}_f$ the flow in the along estuary X direction, the Z structure is that of plane Poiseuille flow with a free surface at $Z = 0$.

$$\mathcal{U}_f = \dot{X} = L(1-Y^2)(1-Z^2)(R+\sin(\pi t)). \tag{4}$$

Due to $\mathcal{U}_f$ being independent of X and the use of the stream function ψ, conservation of volume is satisfied:

$$\frac{\partial \mathcal{U}_f}{\partial X} + \frac{\partial \mathcal{V}_f}{\partial Y} + \frac{\partial \mathcal{W}_f}{\partial Z} = 0. \tag{5}$$

These equations are in the form where the transversal velocity field (i.e. $\mathcal{V}_f$ and $\mathcal{W}_f$) resulting from the secondary circulations is Hamiltonian. However the trajectories evolution has a 3-dimensional element. We think of these equations as like a deck of cards, on which we can have our own separate Poincaré maps. As we evolve through the tidal period these cards are bent, stretched and deformed, though two cards always conserve their X directional separation, due to the fact that $\mathcal{U}_f$ is not a function of X. As we shall explain later, the uncoupled nature of the velocity field means the evolution in the YZ coordinates can be studied in terms of the 2 dimensional Poincaré map.

In the 3 dimensional work that follows we consider the evolution of trajectories starting on a vertical cross section at $X = 0$ (i.e. we consider the behavior of the middle card of the deck). As explained above, all other such cards or vertical cross sections can be considered exact replicas of this and each other. However the cards nearer the X boundaries will be less complete than others, due to the fact that many parts of the card take less time to leave the bounds of the estuary.

We now look at the boundaries to the flow and the dynamics on these boundaries. If we take the velocity fields shown in equations 2, 3 and 4, we find on the boundaries

$$Z = -1, \quad \mathcal{U}_f = 0, \quad \mathcal{V}_f = 0, \quad \mathcal{W}_f = 0, \tag{6}$$

$$\begin{aligned} Z = 0, \quad \mathcal{U}_f &= L(1-Y^2)(R+\sin(\pi t)), \\ \mathcal{V}_f &= (Y^2-1)(1+KY\sin(\pi t)), \quad \mathcal{W}_f = 0, \end{aligned} \tag{7}$$

$$Y = +1, \quad \mathcal{U}_f = 0, \quad \mathcal{V}_f = 0, \quad \mathcal{W}_f = -2Z(1+Z)^2(K\sin(\pi t)+1), \tag{8}$$

$$Y = -1, \quad \mathcal{U}_f = 0, \quad \mathcal{V}_f = 0, \quad \mathcal{W}_f = -2Z(1+Z)^2(K\sin(\pi t)-1). \tag{9}$$

The long term drift of particles on the walls ($Y = \pm 1$) is vertically upwards when $Y = 1$ and vertically downwards when $Y = -1$. There is no X or Y component to any movement on the walls. Trajectories on the bed (i.e. $Z = -1$) of the estuary can not move at all, this is a set of degenerate fixed points. The only place where interesting dynamics may occur is on the free surface of the estuary (i.e. $Z = 0$). Here particles can move both across and along the estuary, with the long term drift however being towards the $Y = -1$ boundary.

2.3. **Scaling to real estuaries.** To scale our model so as to obtain predictions on fluxes etc. for a particular estuary, we have to make certain assumptions. The main assumption is to do with the shape of the estuary's cross section. For volume to be conserved in our scaled version of our model, there must exist no islands within the estuary's bounds. The structures observed in the estuary would therefore be topologically equivalent to those shown in this paper.

The values of scaling parameters we use to scale our model up to the dimensions of a typical partially stratified estuary are,

$$\begin{aligned} H_e = 20m, \quad B_e = 1000m, \quad R_c = 10000m, \quad L = 1 \\ T_e = 12hrs = 43200s, \quad \bar{U} = 0.2ms^{-1}, \quad R = 0.01, \quad K = 11. \end{aligned} \tag{10}$$

Where H_e is the depth of the estuary, B_e is its breadth, T_e is the tidal period, $\bar{U}$ the mean X directional velocity, K is the ratio of the buoyancy driven to the bend driven circulation (K is also approximately equal to the radius of curvature of the estuary R_c divided by the width of the estuary B_e), and R is a value for the ratio of the strength of the component of the velocity field due to the river to that due to the tide. The value of R used may seem very low when first observed, though for an estuary of the type of dimensions we are using it gives 40 tonnes per second fresh water input which is a realistic value. Such parameters are now far removed from the quick mixing assumptions commonly made when modelling estuarine flows, and yet there are still a large class of estuaries (i.e. partially stratified estuaries), which satisfy our conditions.

3. **Transport into and out of regions in YZ.** Here we first explain the connection between the Hamiltonian Poincaré map for YZ and the full 3-dimensional map. We then go on to split the YZ map up into different regions and we finish by connecting these different regions to the patches (ie. differences in concentration) we observe in clouds of pollution.

3.1. **The Poincaré map, a deck of cards.** As we stated earlier we think of the 3-dimensional XYZ space (ie. the whole estuary), at time $t = 0$ as a deck of cards, with the X, along estuary, direction being that of the depth of the pack. Each card in the deck is identical, with the dynamics on each card and its deformation being defined by two different Poincaré maps, or one 3-dimensional Poincaré map. The YZ map controls the dynamics on the card as seen in projection (on to either the $X = -1$ or the $X = 1$ ends of the estuary), while the X map controls how the card is deformed with time. If we were now to evolve our maps over time we would see the deck of cards deform in such a manner that the deformation of each card is identical and the deformation of the deck is just the sum of that of all the individual cards. What is more, if we were to glue the deformed cards together after an arbitrary integer number of periods and then make a new deck of cards by slicing the glued cards vertically, we would find we had exactly the same card (dynamics wise) as the original one at $t = 0$. This means the YZ map governs the YZ dynamics of any arbitrary YZ cross section. This allows us to study the two maps separately, which means we can understand the mixing in the vertical plane independently from that in the horizontal plane. We can therefore obtain a YZ flux from an understanding of the YZ map only.

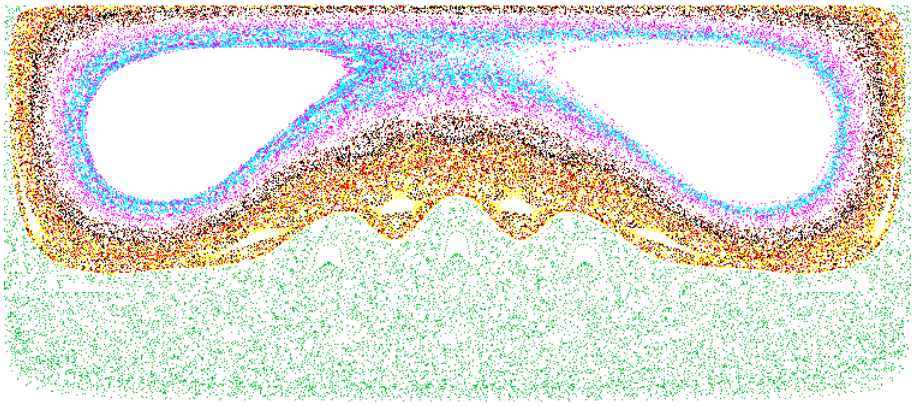

FIGURE 4. The transverse YZ Poincaré map for the velocity field v_f for $K = 11$. This shows the underlying barriers (i.e. the KAM tori) and the partial barriers (cantori) in the estuary's flow. The empty spaces which can be observed are trapped regions around elliptical fixed or periodic points. The upper and lower bounds to the figure correspond respectively to the vertical $Z = 0$ and $Z = -1$ bounds while the left right bounds are respectively the horizontal $Y = -1$ and $Y = 1$ bounds of our model of the estuary.

3.2. **Poincaré maps, turnstile lobes, regions and patchiness.** We now look at the Poincaré map, see figure 4 governing the YZ dynamics. In [21, 31, 11, 14, 12, 27, 28] it is shown in detail how to form partial barriers. It was shown in [21, 31, 14] that the areas of what are known as the turnstile lobes, gives the amount of material moving from one region to the adjacent region across the partial barrier. In a Hamiltonian Poincaré map area is preserved hence the area of both of the turnstile lobes is equal, hence the amount of material entering a region is the same as that leaving.

In figure 5 we see two main partial barriers. The inner barrier corresponds to a partial barrier, formed from segments of stable and unstable manifolds of a hyperbolic fixed point. The outer barrier corresponds to a period 21 approximation of the partial barrier formed by the nearby cantorus. It has been shown that the flux across a cantorus can be approximated by using a nearby periodic orbit with a frequency corresponding to a truncation of the continued fraction expansion of that of the cantorus, [11], see also [14] for a detailed review. This method involves passing an arbitrary curve (see [13]) C_0 between adjacent period n minimizing orbits, via the intermediate period n minimax orbit. This curve is then iterated backwards n times. With the barrier being defined as that formed from the segments of curve corresponding to the original curve C_0 and all its preimages through till the C_{-n+1} preimage. The region between the original curve C_0 and its C_{-n} preimage defines the turnstile lobe and hence the flux across the partial barrier.

We now use these partial barriers and the full barriers formed by the KAM curves to separate YZ space into 7 separate regions, as shown in figure 6. If we bear in mind the different regions that the flow can be separated into and the difference in transport rates or fluxes associated with such regions within the cross section, then we can understand some of the mechanisms for generating patches in a cloud

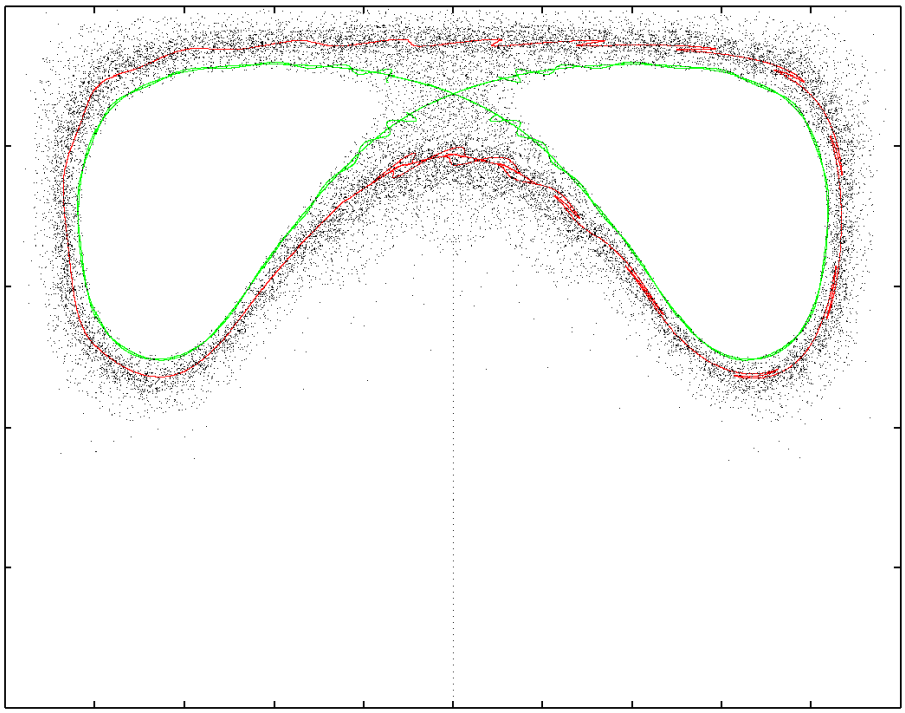

FIGURE 5. Turnstile lobes generated from a period 21 approximation to the two cantori (i.e. seen as bounds to the dark band, in which there is a higher concentration of points) and also the unstable and stable manifolds of a hyperbolic fixed point, $K = 11$.The upper and lower bounds to the figure correspond respectively to the vertical $Z = 0$ and $Z = -1$ bounds while the left right bounds are respectively the horizontal $Y = -1$ and $Y = 1$ bounds of our model of the estuary.

of pollution (i.e. regions of different concentration). We make the claim that the presence of these different structures or regions within the flow would result in the creation of large to intermediate scale patches of higher concentration within clouds of pollution. The smaller regions that could be formed using the high period orbits are, we assume, not seen in the real flow as they are obliterated due to the effect of turbulent fluctuations.

4. **The third dimension: structured but uncoupled.** Here we first introduce the concept of Stokes drift for the X-directional component of a trajectory. We also show how it links in with maps and flows. We then go on to discuss how the regions we see in the YZ map would translate to regions in the flow. We finish by extending the concept of the barriers seen in the 2-dimensional maps to barriers in 3-dimensional flows.

4.1. **Negative Stokes drift, maps and flows.** Here we present the concept of Stokes drift and tie it in with our more dynamics oriented language of maps and flows.

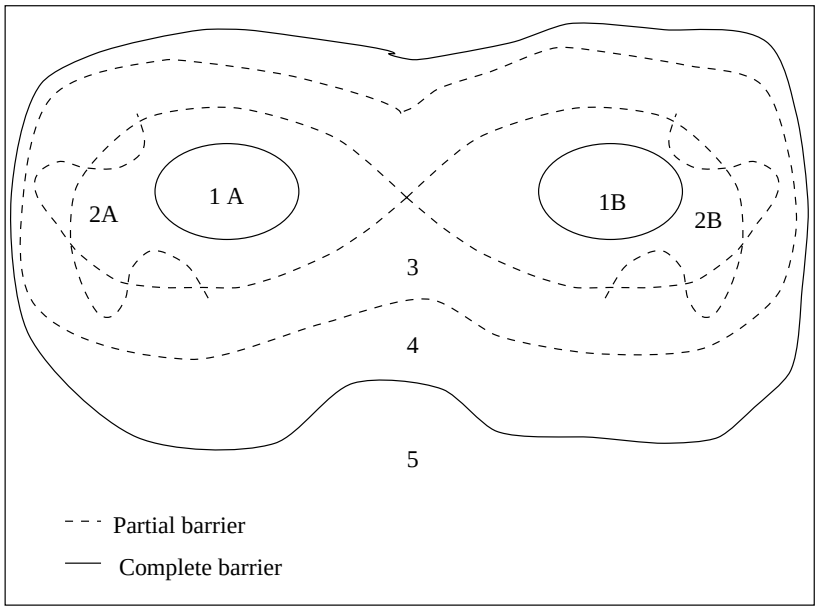

FIGURE 6. This shows the main regions we split the YZ space into. Regions $1A$ and $1B$ are bounded by the KAM curves surrounding the elliptical fixed points. The barrier separating regions $2A$ and 3 and regions $2B$ and 3 is that formed by the unstable and stable manifolds of the hyperbolic fixed point. While the barrier separating regions 3 and 4 is that formed by period 21 approximation to the cantorus. The barrier separating regions 4 and 5 is a KAM curve. The outer bounds to region 5 are the boundaries of the estuary. The upper and lower bounds to the figure correspond respectively to the vertical $Z = 0$ and $Z = -1$ bounds while the left right bounds are respectively the horizontal $Y = -1$ and $Y = 1$ bounds of our model of the estuary.

The Stokes drift is defined as the period averaged movement of particles. (See [18] for an application to transport in an oscillatory tube flow.) A map therefore can be thought of as just a visualization of the Stokes drift. This is because all the map is doing is recording where a particle has evolved to after 1 tidal period, i.e. the Stokes drift. If we observe the Stokes drift in our model we obviously find that it is dependent upon the position of the particle in its YZ coordinates.

If the river flow into the estuary is zero i.e. $R = 0$ (see figure 7) then there is no particular preference for which end of the estuary a particle exits from. A value of the river flow as low as zero could be justified in our model if the estuary was fed by a very small, insignificant, stream.

If we consider the case when $R \neq 0$ (eg. $R = 0.01$), we find that there is definitely a preference as to which end the particles exit from. We also find that most of the particles exit out of the sea end of the estuary and they do so in much less time than for $R = 0$. However we find we can still get a negative, though reduced, Stokes drift for sufficiently small values of R. For larger values of R the Stokes drift due to the flow of the river is such that it overrides any negative Stokes drift due to time

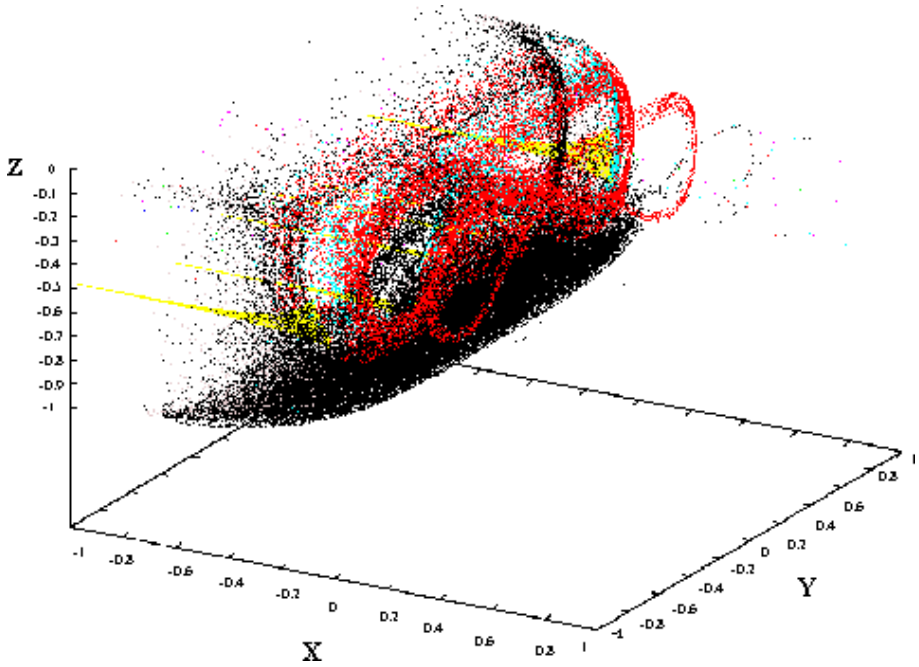

FIGURE 7. The Poincaré map in the full XYZ space, $R = 0$, with different colors representing different orbits. This shows Stokes drift. An example of negative Stokes drift would be the yellow trajectory, while an example of positive Stokes drift would be the red trajectory

periodic estuarine flow. What we would get though is a reduced positive drift in the region of the estuary where previously for a smaller value of R, there had been negative Stokes drift.

For a value of $R = 0.01$ we find that the elliptical fixed point region, (i.e. region $1A$, figure 6), found in the negative half of the cross section (i.e. $Y < 0$), is a region of negative Stokes drift. In our estuary this would correspond to a region found on the outside of the bend, as we can see from the fact that circulation in the single bend driven cell is towards $Y = -1$ (i.e. the outside of the bend).

4.2. **Flows, regions and barriers in 3 dimensions.** Here we concentrate on the structures (i.e. trapping regions, patches etc.) seen in the vertical YZ cross section and show how they would look in 3 dimensions. We study these structures for one initial value of X (i.e. 1 card from a deck of cards) which we shall label X_0. It has to be remembered that due to the lack of an X dependency in equations 2,3 and 4 then other initial values of X will also have the same structures but these structures will be curtailed or extended depending on how close they are to the river ($X = -1$) or sea ($X = 1$) ends of the estuary. The curtailment is because all trajectories with $|X_n| > 1$ (where X_n is the X coordinate of a particle after evolution under the flow for n tidal periods), are considered to have left the estuary.

If all the YZ Poincaré maps are stacked together to obtain the whole 3-dimensional map of the flow in the estuary (i.e. when the cards are collected together to make

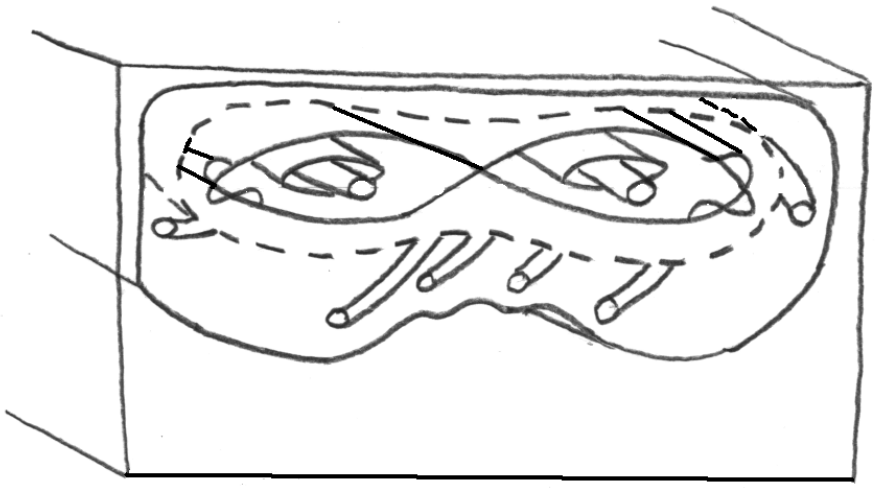

FIGURE 8. Tubes formed as a result of the evolution of the partial and complete barriers observed in the YZ map. The upper and lower bounds to the box (showing a cross section transverse to the along estuary flow) correspond respectively to the vertical $Z = 0$ and $Z = -1$ bounds, while the left and right bounds are respectively the horizontal $Y = -1$ and $Y = 1$ bounds of our model of the estuary. The X along estuary direction is into the page.

the full deck of cards), what we see in the 3 dimensional Poincaré map at an arbitrary time are tubes running in the X direction, see figure 8. The tube-like barriers exist in a slightly more complicated form in the full 3 dimensional flow, however the volume of material which escapes a region defined in the YZ Poincaré map is just the area of the one of the turnstile lobes for that region multiplied by the distance travelled in the horizontal X direction in 1 tidal period. It is these tubes which correspond to the patches observed in clouds of pollution in our estuarine flow.

5. **Predicted fluxes and exit times.** Here we make predictions in YZ space for the vertical fluxes and the exit times (i.e. the time for a trajectory to leave the estuary) for both our model and then scaled up values for our estuary.

5.1. **Theoretical flux or transport rates, for each region in YZ space.** We start by defining the area of a turnstile lobe (i.e. the amount of material leaving or entering a specific region per tidal period) to be a local measurement of flux, κ, see [21, 31, 14]. We term the value of flux for our model, κ_m, and the predicted value for our estuary κ_e. As the area of our cross section in the model is 2, this gives a flux per unit area for our model, $\kappa_{muc} = \frac{\kappa_m}{2}$. This links in with the predicted estuarine flux, κ_e as follows

$$\begin{aligned} \text{predicted flux} &= \frac{\text{width (m) . depth (m) of estuary}}{\text{tidal period (s)}}.\kappa_{muc} \\ \kappa_e &= \frac{B_e.H_e}{T_e}.\frac{A_{tl}^{YZ}}{2} \end{aligned} \tag{11}$$

which for our particular estuaries dimensions, (see equation 10), gives

$$\begin{aligned} \kappa_e &= \frac{1000}{43200}.20.\frac{A_{tl}^{YZ}}{2}(m^2s^{-1}) \\ &= \frac{25}{108}.A_{tl}^{YZ}(m^2s^{-1}). \end{aligned} \tag{12}$$

We found the area A_{tl}^{YZ} of the turnstile lobes in the YZ map to be 1.5×10^{-4} for the turnstile of the homoclinic tangle of the hyperbolic fixed point and 5×10^{-4} for turnstile of the period 21 approximation to the cantori. If we now scale these values, using equation (12), to our particular estuaries dimensions we get fluxes κ_e of $3.5 \times 10^{-5}(m^2s^{-1})$ and $1.2 \times 10^{-4}(m^2s^{-1})$ for the turnstile lobe of the tangle and period 21 orbits respectively.

The fluxes, κ_e for the complete barriers (i.e. those bounding the elliptical regions (i.e. region $1A$ and $1B$, see figure 6) and the large KAM curve separating regions 4 and 5, see figure 6), will obviously be zero due to the nature of the barrier.

5.2. **Exit times.** The question we ask here is, *how many periods does it take, for a particle starting at $X = 0$, Z_0, Y_0 and $t = 0$, to leave the X bounds of the estuary?* We do this by setting up a grid of $2m$ by m points in YZ space and evolving the trajectories under the flow until $|X_n| > 1$. We then record n the number of periods (not necessarily integer), with this being defined to be the exit time for specific space time coordinates. (There is no ambiguity with the notation X_n.) It is important that we make the distinction between a trajectory leaving the estuary under the flow, and one doing so under the mapping. As said before we consider a trajectory to have left the estuary if during the evolution of its trajectory in the flow $|X_n| > 1$. At the sea end, $X = 1$, we consider this to mean the particle has left for ever, while at the river end, $X = -1$, we assume the particle is re-injected back into the estuary. The exit times are then plotted against YZ for $R = 0.01$, see figures 9, and 10. Exit times for the YZ cross section for $R = 0$ were not calculated because they are computationally massive to compute due to the length of the time particles remain within the bounds of the estuary.

If we look at figures 9, and 10 these show some important results. One of the most startling features of these figures is the steps in exit times (i.e. the bands of different color). The position of the steps correspond to that of the partial and complete barriers. This means that

> *the complete and partial barriers do not only separate regions of different mixing, they also separate regions of different Stokes drift and hence different exit times.*

These three concepts: mixing, Stokes drift and exit times, as we shall discuss next, are closely connected. In figures 9 and 10 negative values of n correspond to regions where the particle exited out of the river end of the estuary in n periods. Such regions correspond to regions of negative Stokes drift, which exist for $R = 0$ and can also exist even for $R \neq 0$. The boundary to this region is the partial barrier formed

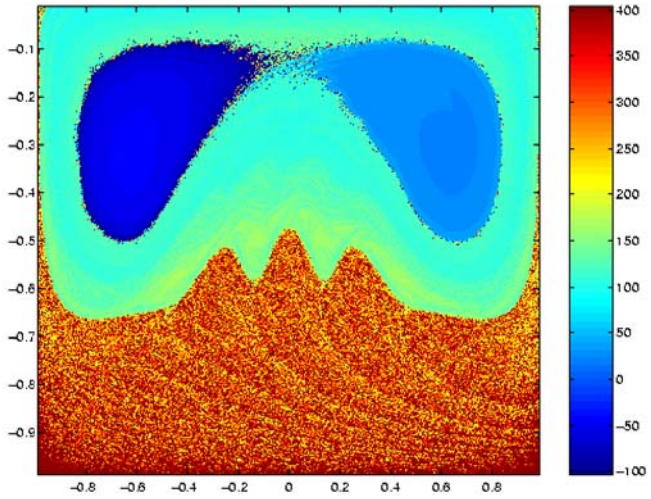

(a.) Exit times, n, for $X = 0$ and $R = 0.01$, seen in projection in YZ space, and color contoured in n. Negative values of n correspond to regions of negative Stokes drift. All values of $n \geq 400$ are colored dark brown, while those values of $n \leq -100$ are colored dark blue.

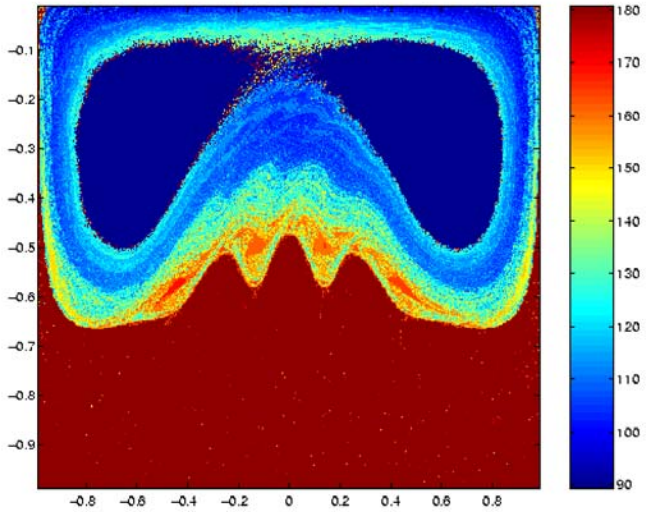

(b.) Exit times, n, for $X = 0$ and $R = 0.01$, focusing in particular on the structure in regions 3 and 4, (see figure 6), by only considering and coloring values of $90 < n < 180$. All values of $n \geq 180$ are colored dark brown, while those values of $n \leq 90$ are colored dark blue.

FIGURE 9. (a) and (b) showing the vertical Z coordinate and the horizontal Y coordinate with the bar showing the relationship between the color and the exit time n.

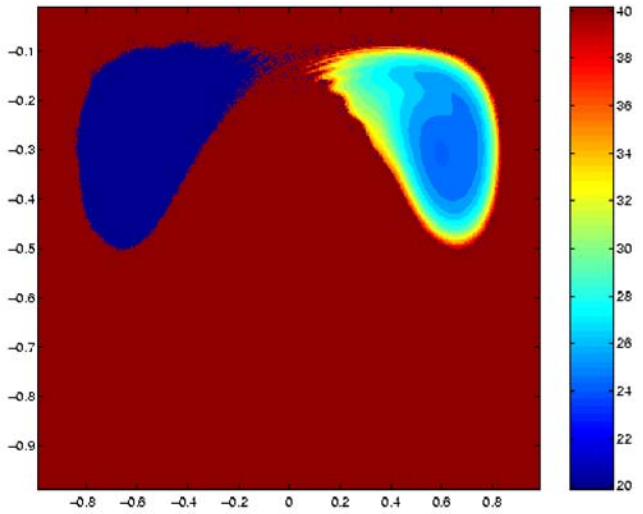

(a.) Exit times, n, for $X = 0$ and $R = 0.01$, focusing in particular on the structure in regions $1B$ and $2B$, (see figure 6), by only considering values of $20 < n < 40$. All values of $n \geq 40$ are colored dark brown, while those values of $n \leq 20$ are colored dark blue.

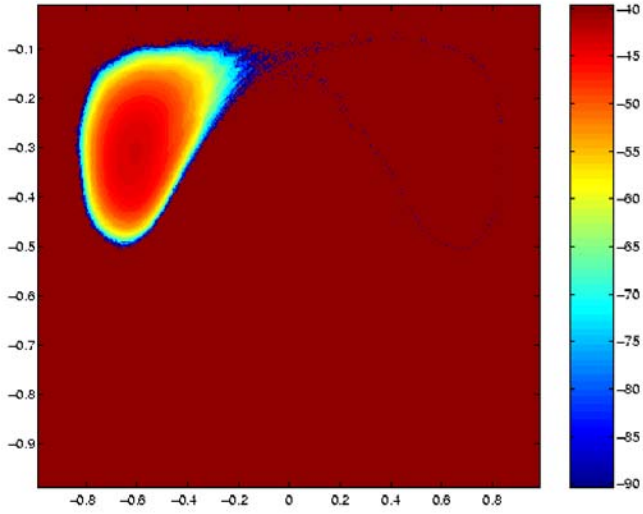

(b.) Exit times, n, for $X = 0$ and $R = 0.01$, focusing in particular on the structure in regions of negative Stokes drift $1A$ and $2A$, (see figure 6), by only considering values of $-90 < n < -40$. All values of $n \geq -40$ are colored dark brown, while those of $n \leq -90$ are colored dark blue.

FIGURE 10. (a) and (b) showing the vertical Z coordinate and the horizontal Y coordinate with the bar showing the relationship between the color and the exit time n.

from the unstable and stable manifolds of the hyperbolic fixed point. Positive Stokes drift refers to regions where n is positive and particles exit the estuary at the sea end.

The most important result we obtain from figures 9 and 10 is that,

> *regions in which the mixing is good and with boundaries which extend close to those of the fluid are regions of long exit time, for flows with non slip boundary conditions.*

In practice such mixing regions are common. They also often the regions where the mixing is best as a result of large velocity differences resulting from the effects of friction at the boundaries of the fluid. We expect this result holds in general for 3-dimensional steady or unsteady, coupled or uncoupled flows (with non-slip boundary conditions) where the third dimension's velocity field is dependent only on the other two dimensions. This is because additional couplings or additional t and X dependencies would not effect the fact that for non slip boundary conditions the flow goes to zero as it approaches the boundary and the resulting large velocity differences generically produce regions of good mixing, but large exit time.

As can be seen from figures 9 and 10, the regions with the smallest exit times are the elliptical fixed point regions. Therefore, if the mixing is good and the regions boundaries extend towards those of the fluid, a particle will experience a wide range of Y and Z values before it leaves the estuary, some of which may result in a large value of the Stokes drift and some of which may result in a small or even a negative value of the Stokes drift, hence resulting in a reduced overall drift. If the mixing is poor and the region does not extend close to the boundaries, as is the case for particles trapped in the elliptical fixed point regions, the particle will experience a much smaller range of Y and Z values, and as it remains far from the boundaries a much more constant positive or negative drift, resulting in smaller exit times, (i.e. the converse of our second result is also true).

What can also be seen from figures 9 and 10 if one looks closely is that there are also regions (i.e. the high order periodic islands, on either side of the KAM curve) in we have poor mixing and due to the proximity of the fluids boundary we have large exit times. One can also see that there is an asymmetry for exit times for the two elliptical fixed point regions. The region which exits out into the river (i.e. the region of negative n) does so slower than the region exits out into the sea. This is due to fact that the flow exiting out of the river end has to drift against the river's component of the estuarine flow.

If we consider how the exit times picture would look for the full XYZ space, we find that differences in X_0, the initial value of X, would not lead to simple proportional differences in n. This is due to the YZ dependency of X directional component of the full 3-dimensional velocity field. We would therefore have to build an exit-time map for the full XYZ space or at least the specific X coordinates of interest to fully understand the problem.

6. **Summary including practical implications: Optimal discharge sites, patchiness and diffusion.**

In this section we summarize our results for the predicted fluxes and exit times and then use them to make predictions as to what we expect to see in an estuary which fits our assumptions. We then go onto discuss exit times and what they mean for the material being flushed out of an estuary. We

finish by making recommendations for the optimal discharge coordinates for a pollution outfall site, and suggesting policies to insure that the discharge of pollution remains optimal over the tidal period.

6.1. **Fluxes and barriers.** Our analysis gives a lower bound for the fluxes within a cloud of pollution. This is because the curves we have used to find these fluxes are curves of minimal flux. See [11, 12, 14]. In other words we have picked out the main barriers, partial or complete, to transport. As can be seen from the Poincaré maps, figures 4, 5 and the schematic, figure 6, these barriers create trapping regions. We equate these trapping regions to regions or patches of higher concentration within a cloud of pollution. In our analysis so far we have omitted the effects of molecular diffusion and turbulent fluctuations. This is also another reason why our results are a lower bound.

What we expect to see in a flow in the type of estuary we are modelling (i.e. a partially stratified estuary and not a well mixed one) is the presence of tube-like structures of a higher or lower concentration than the mean for a particular cloud of pollution. See figures 8. The barriers to these tube-like structures would be the partial and complete barriers we observe in our model. However, when we add the effect due to turbulent fluctuations and molecular diffusion we will find that the transport across these barriers has increased, and therefore we no longer get complete barriers.

As we stated in the previous section, the fluxes associated with different barriers in the template of the turbulent flow are either very low (i.e. of the order 10^{-4} and $10^{-5}m^2s^{-1}$), or zero, for the complete barriers. In the short time scale this means that the main means of crossing these barriers, be they partial or not, must come from either the effects of turbulent or molecular diffusion. However the transport due to molecular diffusion is insignificant, being only of the order $10^{-9}m^2s^{-1}$, (see [3]). The means of escape from the regions enclosed by our partial and complete barriers is therefore essentially due to the effects of turbulent diffusion (see [6, 25] and references there in for a discussion on turbulent diffusion in estuarine flows). This diffusivity adds a fuzziness to the Poincaré maps we generate. However the structures which are observed in the Poincaré map of our template still underly the dynamics in the map of the full estuarine flow V. We would therefore expect in the short time scale to see a fuzzy version of the tubes and barriers that we observed in the model in the turbulent flow.

6.2. **Optimal discharge regions in the YZ plane.** As we described earlier, and as can be seen from figures 9 and 10, the exit times are smallest in regions $1A$ and $1B$. (See figure 6.) Region $1A$ is on the outside of the bend and discharges out of the river end and region $1B$ is on the inside of the bend and discharges out of the sea end of the estuary. The other four regions can be ordered from 2 through to 5 consecutively in order of increasing exit times. The problem is however, as we concluded in section 6, that the regions where the exit time is smallest are regions of poor mixing. In such regions the mixing is essentially due to the random effects of turbulent diffusion. The regions where the mixing is better have larger exit times.

To propose an optimal site for the discharge of pollutants we have to optimize the exit time and the mixing. We have to decide whether we want either good mixing and poor exit times or poor mixing and good exit times, or indeed somewhere in between. We also have to understand the following two questions for our flow. First, *what effect would turbulent diffusion have on the exit times?* Second, *what*

effect would gravity have on the exit time, if the density of the pollution was not equal to that of the water in the estuary?

We consider the first question. Addition of a turbulent diffusion to the flow has the effect of increasing the effective mixing for a specific region of the cross section. This means that particles could escape regions more easily and therefore the likelihood of their trajectories encountering regions where the drift was very slow would increase. The end result is, in general, an increase in the exit times, with the stronger the turbulent diffusion the greater, in general, the increase in the exit time.

We now consider the second question. If the density of the pollution in a cloud was greater than that of the water in the estuary, then the overall effect would be for the cloud to sink towards the bed of the estuary. This means that the cloud would sink into a region where the exit times are greater, and ultimately the cloud will sink to the bed of the estuary where the exit time is effectively infinite. Therefore the effect of a pollution cloud containing particles with a density greater than the water in the estuary is to increase the exit time. The greater the density difference the greater the increase in the exit time. The effect of a pollution cloud being less dense than that of the estuary's water would be to make the cloud rise in the flow. This would therefore, in general, result in a decrease in the time taken to exit, hence giving a smaller exit time, in general. As can be seen from figures 9 and 10 in general the higher up we are in the flow the quicker the exit time.

The most important use of these results is in indicating *where and when and also, where not and when not, to discharge pollution in to our estuary.* We start by indicating the black spots, i.e. the places where it is definitely not a good idea to discharge pollution. As can be seen from figures 9 and 10, three regions have either a negative Stokes drift and hence result in a drift of pollution back up the estuary (regions $1A$ and $2A$) or have potential for such a slow exit, so that in effect the pollution may never leave the estuary (region 5). These are obviously the regions where the discharge of pollution should definitely be avoided. This leaves regions $1B$, $2B$, 3 and 4. Of these four regions region $1B$ is elliptical and hence the mixing in this region is due to the effects of turbulent diffusion alone. This region has the smallest exit times, but the discharge of pollution into such regions would be undesirable due to the fact that the pollution would dilute at such a slow rate, depending on the strength of the turbulent diffusion. Effectively all that would be happening in such a region, in the short time scale, is that the pollution would be transported down the estuary to another place at approximately the same concentration at which it was discharged into the estuary. Region $2B$ is the region with the second smallest exit time, this region is a chaotic region and hence a region where the mixing will be better than in region $1B$. The problem with this region however is that the diffusion across the barriers surrounding it is essentially due only to turbulent diffusion due to the fact that the area of the turnstile lobe is so small. Also the size of region $2B$ is quite small in comparison to regions 3 and 4, therefore the dilution of the pollutant will not be large and the chance of actually discharging into it and not one of its neighbours is small (at least for an estuary with a vertical cross section shaped similar to that in our model). This therefore leaves regions 3 and 4 for regions in which to place the optimal discharge site. Of these we recommend region 4 as the exit times for both regions are about the same and region 4 is the furthest away from potential sources of trouble, such as the negative Stokes drift in region $2A$.

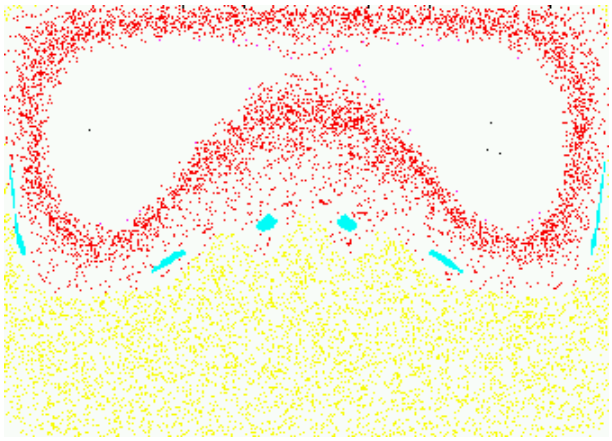

(a)YZ Poincaré map, $t_0 = 0$.

(b)YZ Poincaré map, $t_0 = T/4$.

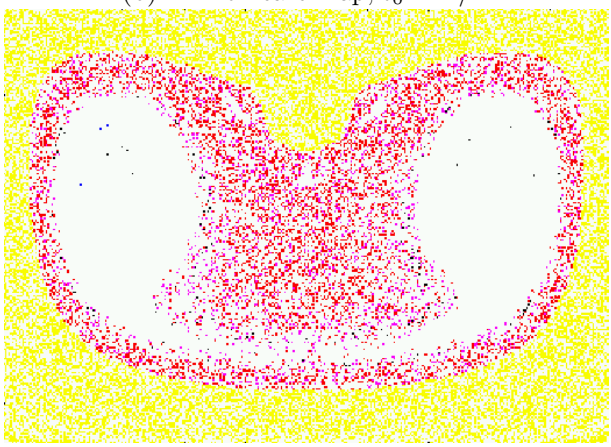

(c)YZ Poincaré map, $t_0 = T/2$.

FIGURE 11. YZ Poincaré maps, (a), (b) and (c) for $t_0 = 0, T/4$, and $T/2$. respectively, where T is the tidal period and $K = 11$. The upper and lower vertical bounds to the figures are $Z = 0$ and $Z = -1$ respectively, while the left and right bounds are $Y = -1$ and $Y = 1$ respectively.

These recommendations could change if we were to scale our model to a much different shaped estuary. The choice of optimal region however would still be between regions $2B$, 3 and 4.

6.3. **Optimal discharge coordinates in space and time.** Having in the previous subsection just picked region 4 as the optimal discharge region we have to now give coordinates in space and time for our discharge site. If we are wanting to flush pollution out of the estuary and we are in a place of positive Stokes drift then the closer the discharge site is to the sea end $X = 1$, the better. If we were instead to hit a region of negative Stokes drift however, then near the sea end barrier would be one of the worst places. This would result in the pollution travelling all the way back up the estuary and if the region was elliptical, it would do so in a relatively undiluted manner.

The final coordinate we need to account for is time. This is important as can be seen from figures 11 a, b, and c, the actual position in the vertical cross section of the regions 1 to 5 changes during one tidal period. This means what could be an optimal site for discharge at one time could periodically be a very poor site at another time within the same tidal period.

We can deal with the problem of the moving regions in a few ways. The first way would be to find an outfall site that remained in the desired region for the whole period. This appears to be unlikely from the Poincaré maps (figures 11). Another simple way could be to not discharge pollution when the outfall site is not in the optimal region. This would involve the use of small holding tanks to hold the pollution for a time until it was safe to discharge it again. The final solution would be to develop a strategy for releasing the pollution which kept the effective discharge site in the optimum region. By effective discharge site we mean the site at which the pollution behaves as though it has been discharged from. In other words we mean that we discharged the pollution at a particular site, not the optimum one, but we do so at a velocity, or even density, which causes the pollution to behave as though it were discharged from the optimum site. We could then control the release of pollution from our non optimum outfall site in such a manner so as to cause the effective discharge site to always be in the optimum region (i.e. region 4). Such a policy may well be difficult though not impossible to execute. It may also be the only solution for the minimization of the environmental impact of an existing non optimal discharge site.

Acknowledgements

This work and my stay in Barcelona was supported by Centre Recerca Matemática, Bellaterra, Spain and the grant SB2000 − 0075 from the Secretaría de Estado de Educación y Universidades and Fondo Social Europes. I would like to thank Ron Smith and Cecil Scott for many helpful discussions. I would also like to acknowledge parents, grandparents.

REFERENCES

[1] H.F. Aref, "Stirring by chaotic advection," J. Fluid Mech. **143** (1984), 1-21.

[2] H.F. Aref, Guest editor "Chaos applied to fluid mixing," Chaos Solitons and Fractals, **4** 6 1994.

[3] G.K. Batchelor,"An introduction to fluid dynamics" Cambridge University press, Cambridge, 1967, 595.

[4] P.C. Chatwin and C.M. Allen, "Mathematical models of dispersion in rivers and estuaries," Ann. Rev. Fluid Mech. **17** (1985), 119-149.

[5] R. Dorrestein, "On the distribution of salinity and of some other properties in the water of the Ems estuary," Verh. K. ned. geol.-mijnd. Genoot., **19** (1960), 43-74.
[6] H.B. Fischer, "Longitudinal dispersion and turbulent mixing in open channel flow," Ann. Rev. Fluid Mech. (1973), 59-78.
[7] H.B. Fischer, "Mixing and dispersion in estuaries," Ann. Rev. Fluid Mech. 8 (1976), 107-133.
[8] H.B. Fischer, N.H.Brooks, J. Imberger, R.C.Y Koh, and E.J. List, "Mixing in Inland and Coastal Waters," Academic Press, New York, 1979.
[9] I. Guymer, and J.R. West, "Field studies of the flow structure in a straight reach of the Conwy estuary," Estuarine, Coastal and Shelf Science, **32** (1991), 581-596.
[10] I. Guymer, and J.R. West, "Longitudinal dispersion coefficients in estuary," Journal of Hydraulic Engineering, **118** (1992), No. 5.
[11] R.S. MacKay, J.D. Meiss, and I.C. Percival, "Transport in Hamiltonian systems," PhysicaD **13** (1984), 55-81.
[12] R.S. MacKay, "Transport in 3D volume-preserving flows," J. Nonlinear Sci. **4** (1994), 329-354.
[13] J.N. Mather, "Existance of quasi-periodic orbits for twist homeomorphisms of the annulus," Topology, **21** (1982), 457-467.
[14] J.D. Meiss, "Symplectic maps, variational principles, and transport," Reviews of Modern Physics, **64** (1992), 795-848.
[15] R.A. Nunes, and J.H. Simpson, "Axial convergence in a well-mixed estuary," Estuarine, Coastal and Shelf Science, **20** (1985), 637-649.
[16] J.M. Ottino, "The Kinematics of Mixing: Stretching, Chaos and Transport," Cambridge University Press. Cambridge, 1989.
[17] R. Pasmanter, "Dynamical systems, deterministic chaos and dispersion in shallow tidal flows," in Physical Processes in Estuaries pp. 42-52. Springer, Heidelberg, 1988.
[18] T.J. Pedley, and R.D. Kamm, "The effect of secondary motion on axial transport in oscillatory tube flow," J. Fluid Mech., **193** (1988), 347-367.
[19] H. Postma, "The distribution of temperature and salinity in the Wadden Sea," Tijdscr. K. ned. aardrijksk. Genoot., **67** (1950), 34-42.
[20] H. Ridderinkhof, and J.F.T. Zimmerman, "Chaotic stirring in a tidal system," Science, **258** (1992), 1107-1111.
[21] V. Rom-Kedar, S. Wiggins," Transport in two-dimensional maps," Archive for Rational Mech. and Anal. **109** 3 (1990), 239-298.
[22] C. Scott, "A numerical study of the interaction of tidal oscillations and non-linearities in an estuary" Estuarine, Coastal and Shelf Science, **39** (1994), 477-496.
[23] R. Smith, "Longitudinal dispersion of a buoyant contaminant in a shallow channel," J. Fluid Mech., **78** (1976), 4, 677-688.
[24] R. Smith, "Longitudinal dispersion of contaminants in small estuaries," J. Fluid Mech., **82** (1976), 1, 129-146.
[25] R. Smith, "Multi-mode models of flow and of solute dispersion in shallow water. Part 3. Horizontal dispersion tensor for velocity" J. Fluid Mech., **352** (1997), 331-340.
[26] R. Smith and C. Scott, "Mixing in the tidal environment," Journal of Hydraulic Engineering, **123** (1997), 4, 332-340.
[27] J.R. Stirling, "Painting pictures of turbulence: chaotic advection and transport in $(3+1)$-dimensional flows." Ph.D Thesis, Department of mathematical Sciences, Loughborough University, UK, 1998.
[28] J.R. Stirling, "Transport and bifurcation in a non-area preserving 2-D map with applications to the discharge of pollution in an estuarine flow." PhysicaD 144 (2000), 169-193.
[29] J.W. Talbot and G.A. Talbot, "Diffusion in shallow seas and in English coastal and estuarine waters," Rapp. P-v. Reun. Cons. int. Explor. Mer., **167** (1974), 93-110.
[30] J.R. West, and J.S. Mangat, "The determination and prediction of longitudinal dispersion coefficients in a narrow, shallow estuary," Estuarine, Coastal and Shelf Science, **22** (1986), 161-181.
[31] S. Wiggins, "Chaotic Transport in Dynamical Systems," Interdisciplinary Applied Mathematics, Springer-Verlag, Berlin, 1992.

Received February 2002; revised June 2002; final version December 2002.

E-mail address: j.r.stirling@mailcity.com